The Astrophysical Journal Letters, 722:L54–L57, 2010 October 10 doi:10.1088/2041-8205/722/1/L54

C_{60} IN REFLECTION NEBULAE

Kris Sellgren[1], Michael W. Werner[2], James G. Ingalls[3], J. D. T. Smith[4], T. M. Carleton[5], and Christine Joblin[6,7]
[1] Department of Astronomy, Ohio State University, Columbus, OH 43235, USA; sellgren@astronomy.ohio-state.edu
[2] Jet Propulsion Laboratory, California Institute of Technology, Pasadena, CA 91109, USA
[3] Spitzer Science Center, California Institute of Technology, Pasadena, CA 91125, USA
[4] Ritter Astrophysical Research Center, University of Toledo, Toledo, OH 43603, USA
[5] Steward Observatory, University of Arizona, Tucson, AZ 85721, USA
[6] Université de Toulouse, UPS, CESR, 9 ave colonel Roche, F-31028 Toulouse cedex 4, France
[7] CNRS, UMR 5187, 31028 Toulouse, France
Received 2010 August 6; accepted 2010 September 2; published 2010 September 17

ABSTRACT

The fullerene C_{60} has four infrared-active vibrational transitions at 7.0, 8.5, 17.4, and 18.9 μm. We have previously observed emission features at 17.4 and 18.9 μm in the reflection nebula NGC 7023 and demonstrated spatial correlations suggestive of a common origin. We now confirm our earlier identification of these features with C_{60} by detecting a third emission feature at 7.04 ± 0.05 μm in NGC 7023. We also report the detection of these three C_{60} features in the reflection nebula NGC 2023. Our spectroscopic mapping of NGC 7023 shows that the 18.9 μm C_{60} feature peaks on the central star and that the 16.4 μm emission feature due to polycyclic aromatic hydrocarbons peaks between the star and a nearby photodissociation front. The observed features in NGC 7023 are consistent with emission from UV-excited gas-phase C_{60}. We find that 0.1%–0.6% of interstellar carbon is in C_{60}; this abundance is consistent with those from previous upper limits and possible fullerene detections in the interstellar medium (ISM). This is the first firm detection of neutral C_{60} in the ISM.

Key words: ISM: individual objects (NGC 7023, NGC 2023) – ISM: lines and bands – ISM: molecules – line: identification

1. INTRODUCTION

Fullerenes are cage-like molecules (spheroidal or ellipsoidal) of pure carbon such as C_{60}, C_{70}, C_{76}, and C_{84}. C_{60}, also known as buckminsterfullerene, is the most stable fullerene and can account for up to 50% of the mass of fullerenes generated in the laboratory (Kroto et al. 1985). Theorists have suggested that fullerenes might form around stars with carbon-rich atmospheres such as carbon stars, Wolf–Rayet (WC) stars, and carbon-rich, hydrogen-poor R Cr B stars (Kroto & Jura 1992; Goeres & Sedlmayr 1992; Cherchneff et al. 2000; Pascoli & Polleux 2000). Fullerenes may also form as part of the carbon-rich grain condensation process known to occur in the ejecta of Type II supernovae (Clayton et al. 2001). Hydrogenated amorphous carbon grains in the interstellar medium (ISM) may also decompose after interstellar shocks into polycyclic aromatic hydrocarbons (PAHs) and fullerenes (Scott et al. 1997); PAHs comprise 9%–18% of interstellar carbon (Joblin et al. 1992; Tielens 2008). Fullerenes might also form via cold interstellar gas-phase chemistry (Bettens & Herbst 1996, 1997).

Foing & Ehrenfreund (1994) propose that two diffuse interstellar bands at 958 and 963 nm are due to singly ionized C_{60}, or C_{60}^+, although the identification is debated (Maier 1994; Jenniskens et al. 1997). Misawa et al. (2009) attribute additional diffuse interstellar bands at 902, 921, and 926 nm to C_{60}^+. No fullerenes were found toward carbon-rich post-asymptotic giant branch stars (Somerville & Bellis 1989; Snow & Seab 1989), carbon stars (Clayton et al. 1995; Nuccitelli et al. 2005), or R CrB stars (Clayton et al. 1995; Lambert et al. 2001). Cami et al. (2010) have recently detected C_{60} and C_{70} in the planetary nebula Tc 1 (IC 1266).

Observational evidence for neutral fullerenes in the ISM, however, has been elusive to date. No neutral fullerenes have yet been found in the diffuse ISM (Snow & Seab 1989; Herbig 2000), dense molecular clouds (Nuccitelli et al. 2005), or at the photodissociation front in the reflection nebula NGC 7023 (Moutou et al. 1999).

C_{60} has four infrared-active vibrational transitions at 7.11, 8.55, 17.5, and 19.0 μm at 1200 K (gas phase; Frum et al. 1991), and at 6.98, 8.44, 17.3, and 18.9 μm at 2.4 K (para-H_2 matrix isolation; Sogoshi et al. 2000). On this basis, we tentatively identified the 17.4 and 18.9 μm ISM emission features in the reflection nebula NGC 7023 as due to C_{60} (Werner et al. 2004b; Sellgren et al. 2007).

We provide here additional evidence for the presence of C_{60} in reflection nebulae. We report here the detection of the predicted C_{60} feature at 7.04 ± 0.05 μm in NGC 7023. We also report the detection of C_{60} features at 7.04, 17.4, and 18.9 μm in a second reflection nebula, NGC 2023. The C_{60} 8.5 μm feature is too blended with strong 8.6 μm PAH emission to be detected in reflection nebulae. We have found in NGC 7023 (Sellgren et al. 2007) that the 16.4 μm emission feature, attributed to PAHs (Moutou et al. 2000), has a spatial distribution distinct from that of the 18.9 μm emission feature. We now compare the spatial distributions of the 16.4, 17.4, and 18.9 μm emission features in NGC 7023 and find additional support for the C_{60} identification. We also discuss the excitation mechanism for the infrared emission of C_{60}.

2. OBSERVATIONS

We used the *Spitzer Space Telescope* (Werner et al. 2004a) with the Infrared Spectrograph (IRS; Houck et al. 2004) to obtain 5–38 μm spectra of NGC 2023 (PI: Sellgren, pid 40276, aorkeys = 23912704, 23911168) and NGC 7023 (PI: Sellgren, pid 40276, aorkeys = 23911424, 23911680). We obtained spectra with the short-wavelength low-resolution module SL (5–14 μm; $\lambda/\Delta\lambda$ = 60–120), the long-wavelength low-resolution module LL (14–38 μm; $\lambda/\Delta\lambda$ = 60–120), and the short-wavelength high-resolution module SH (9.5–19.5 μm;

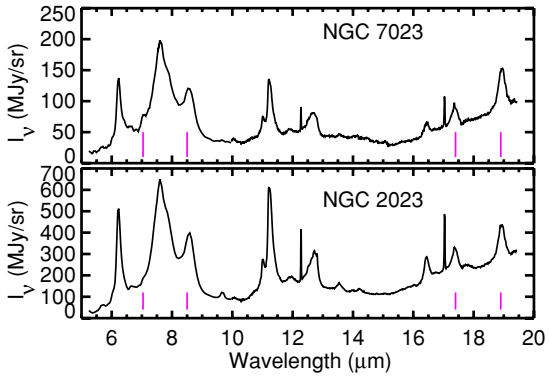

Figure 1. *Spitzer*-IRS spectra (solid curves) of NGC 7023 (25″ east, 4″ north of HD 200775; top) and NGC 2023 (29″ west, 8″ south of HD 37903; bottom), obtained with the short-wavelength low-resolution module (SL; 5.2–10.0 μm; $\lambda/\Delta\lambda$ = 60–120) and the short-wavelength high-resolution module (SH; 10.0–19.5 μm; $\lambda/\Delta\lambda = 600$). We mark C_{60} lines at 7.04, 8.5, 17.4, and 18.9 μm (vertical lines). The strong emission feature at 8.6 μm is due to PAHs. H_2 emission lines fall at 9.66, 12.3, and 17.0 μm.

$\lambda/\Delta\lambda = 600$). We chose nebular positions (29″ west, 8″ south of HD 37903 in NGC 2023; 25″ east, 4″ north of HD 200775 in NGC 7023) with a strong ratio of the 18.9 μm feature relative to the 16.4 μm PAH feature. We used matched aperture extraction in CUBISM (Smith et al. 2007b) to extract SL, LL, and SH spectra in regions of overlap between these spectral modules. The extraction aperture was $10\farcs2 \times 10\farcs2$ in NGC 2023 and $7\farcs5 \times 9\farcs2$ in NGC 7023.

We also retrieve from the *Spitzer* archive a spectral data cube for NGC 7023 with LL (PI: Joblin, pid 3512; aorkey = 0011057920). We use CUBISM to derive spectral images in the 16.4, 17.4, and 18.9 μm features and 0–0 S(1) H_2 for NGC 7023. For the spectrum of each spatial pixel, we define a local continuum surrounding an emission feature or line and subtract it before deriving the feature or line intensity.

We search for bad pixels and correct them with CUBISM before extracting final spectra. We subtract dedicated sky spectra for the 5–38 μm spectra of NGC 2023 and NGC 7023; no sky subtraction is done for the spectral mapping.

3. RESULTS

Figure 1 illustrates our SL and SH spectra in NGC 2023 and NGC 7023. The 17.4 and 18.9 μm emission features are prominent and coincident with C_{60} wavelengths.

We show the 5–9 μm SL spectrum of NGC 7023 in Figure 2. We clearly detect an emission feature at 7.04 ± 0.05 μm. This feature is coincident, within the uncertainties, with the wavelength of the expected C_{60} line. We highlight this emission feature by using PAHFIT (Smith et al. 2007a) to fit the 5–9 μm spectrum with a blend of PAH emission features in addition to the new emission feature at 7.04 μm. The full-width at half-maximum of the 7.04 μm C_{60} feature is 0.096 ± 0.012 μm, significantly broader than our spectral resolution. We also detect the 7.04 μm C_{60} feature in NGC 2023. We present the C_{60} band intensities in Table 1.

In our previous long-slit spectroscopic investigation of NGC 7023 (Sellgren et al. 2007), we found that the 18.9 μm feature peaks closer to the central star than PAHs. We now illustrate this more clearly with the LL spectroscopic map extracted in NGC 7023 (Figure 3). The 18.9 μm emission is clearly centered on the star. By contrast, the 16.4 μm PAH emission peaks outside the region of maximum 18.9 μm emission, in a layer

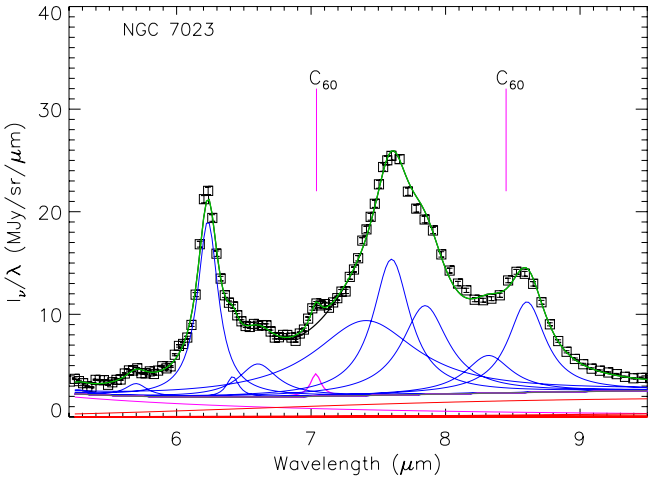

Figure 2. *Spitzer*-IRS 5–9 μm spectrum of NGC 7023 (open squares), obtained with the short-wavelength low-resolution module (SL; $\lambda/\Delta\lambda$ = 60–120). We mark C_{60} lines at 7.04 and 8.5 μm (vertical lines). We show the individual contributions of PAH features at 5.3, 5.7, 6.2, 6.4, 6.7, 7.4, 7.6, 7.8, 8.3, and 8.6 μm to the spectrum, by decomposing the spectrum with PAHFIT (Smith et al. 2007a) and then overplotting the Drude profile of each feature (blue curves). The Drude fit to the C_{60} feature we detect at 7.04 ± 0.05 μm is highlighted (magenta curve). The 8.5 μm C_{60} feature is blended with the strong 8.6 μm PAH feature.

Table 1
Observed[a] and Calculated[b] C_{60} Intensity Ratios[c]

	$I_{7.04}/I_{18.9}$	$I_{8.5}/I_{18.9}$	$I_{17.4}/I_{18.9}$
Object			
NGC 7023 ($\lambda/\Delta\lambda$ = 60–130)	0.82 ± 0.12	···	0.42 ± 0.02
NGC 7023 ($\lambda/\Delta\lambda$ = 600)	···	···	0.33 ± 0.01
NGC 2023 ($\lambda/\Delta\lambda$ = 60–130)	0.086 ± 0.004	···	0.47 ± 0.01
NGC 2023 ($\lambda/\Delta\lambda$ = 600)	...	...	0.66 ± 0.01
Absorbed photon energy			
5 eV	0.46–0.58	0.41–0.43	0.28–0.38
10 eV	0.76–0.94	0.57–0.59	0.28–0.38
15 eV	0.97–1.20	0.67–0.71	0.29–0.38

Notes.
[a] Observed intensity ratios, derived using PAHFIT (Smith et al. 2007a). We give statistical uncertainties; systematic fitting uncertainties are 15% for the 7.04 μm intensity ratio and 30% for the 17.4 μm intensity ratio. The observed 17.4 μm feature has not been corrected for PAH emission blended with it.
[b] Emission spectrum calculated with Monte Carlo code (Joblin et al. 2002) for molecular cooling cascade after absorbing a stellar photon. C_{60} vibrational data from Ménendez & Page (2000), Choi et al. (2000), and Schettino et al. (2001).
[c] Intensities (W m^{-2} sr^{-1}) normalized to the 18.9 μm feature intensity.

between the star and the molecular cloud. The photodissociation front at the UV-illuminated front surface of the molecular cloud is delineated by 0–0 S(1) H_2 emission at 17.0 μm.

Our previous observations (Sellgren et al. 2007) suggested that the 17.4 μm feature might be a blend of a PAH feature and an emission feature with the same spatial distribution as the 18.9 μm feature. We now confirm that this is the case with IRS/LL spectroscopic imaging. We show an image of the 17.4 μm emission from NGC 7023 in Figure 4, overlaid with contours of 18.9 μm and 16.4 μm emission. The 17.4 μm emission clearly shows one peak on the central star, coincident with 18.9 μm C_{60} emission, and a second peak cospatial with 16.4 μm PAH emission. Thus, there is an ISM component with emission features at 17.4 and 18.9 μm, which has a different spatial distribution than PAHs traced by the 16.4 μm feature.

Our imaging spectroscopy demonstrates the spatial separation between regions of peak PAH emission and peak C_{60} emission

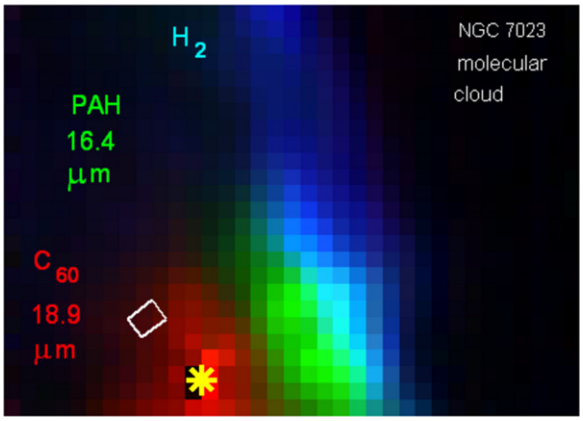

Figure 3. Three-color image of NGC 7023, in 18.9 μm C_{60} emission (red), 16.4 μm PAH emission (green), and 17.0 μm 0–0 S(1) H_2 emission (blue). We constructed each image by analyzing *Spitzer*/IRS-LL long-slit spectra with CUBISM (Smith et al. 2007b). We illustrate where we measured the 5–38 μm spectra shown in Figures 1 and 2 (white rectangle). We mark the location of HD 200775 (star). Each pixel is 5.″1 × 5.″1. The 18.9 μm C_{60} feature peaks on the central star, while the 16.4 μm PAH emission is brightest between the 18.9 μm emission region and the photodissociation front traced by H_2 emission.

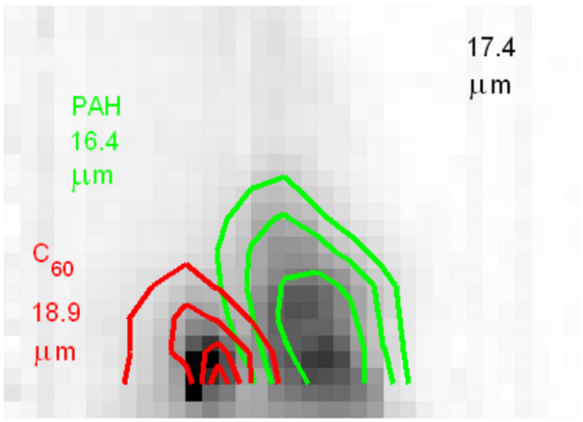

Figure 4. Image of 17.4 μm emission in NGC 7023 (grayscale image), derived from *Spitzer*/IRS-LL long-slit spectra analyzed with CUBISM (Smith et al. 2007b). We overlay contours of 18.9 μm C_{60} emission (red) and 16.4 μm PAH emission (green). Each pixel is 5.″1 × 5.″1. One component of the 17.4 μm emission is cospatial with 18.9 μm C_{60} emission and the other component of the 17.4 μm emission follows 16.4 μm PAH emission. This illustrates that the 17.4 μm emission feature is a blend of a PAH feature and 17.4 μm C_{60} emission.

(Figures 3 and 4). Boersma et al. (2010) find that the 16.4 μm feature from different sources correlates with other PAH features but the 18.9 μm feature does not. Velusamy & Langer (2008) observe the 18.9 μm feature to peak on the central star in the reflection nebula NGC 2316 (Parsamian 18). They also find that the 17.4 and 18.9 μm features have distinct spatial distributions in this object and argue from this that C_{60} is unlikely to be the carrier of these features. Our result that the 17.4 μm feature is a blend of a PAH feature and C_{60} in NGC 7023 naturally explains their observations.

4. DISCUSSION

To derive the abundance of C_{60}, we assume that fullerenes and PAHs absorb UV starlight, and then re-radiate it all as infrared emission features. We do not include any potential visible fluorescence by either C_{60} or PAHs. For fullerenes, we adopted experimental values of the absorption cross-section of C_{60} at 0.09–0.35 μm (Yasumatsu et al. 1996; Yagi et al. 2009). The absorption cross-sections from Yasumatsu et al. (1996) and Yagi et al. (2009) differ by a factor of two, indicating the overall uncertainty in our abundance calculation. For PAHs, we adopted the absolute absorption cross-section at 0.09–0.30 μm from Li & Draine (2001). We integrated both of these absolute absorption cross-sections over a 17,000–22,000 K blackbody, as is appropriate for the central stars of NGC 7023 and NGC 2023. We find that C_{60} and PAHs have similar integrated UV absorption strengths per C atom.

We compare the sum of the intensities of the 7.04, 17.4, and 18.9 μm features, assumed to be due to C_{60}, to the sum of all other infrared emission features at 5–38 μm, assumed to be due to PAHs. We analyze SL and LL spectra with PAHFIT (Smith et al. 2007a) to find that the ratio of C_{60} to PAH emission is 0.01–0.03 in our observed positions in NGC 7023 and NGC 2023. By adopting a percentage of interstellar carbon in PAHs of 9%–18%, we derive a percentage of interstellar carbon in C_{60}, $p(C_{60})$, of 0.1%–0.6% in regions of bright C_{60} emission.

Our $p(C_{60})$ value is consistent with other estimates of $p(C_{60})$ and of the percentage of carbon in C_{60}^+, $p(C_{60}^+)$. Foing & Ehrenfreund (1994) estimate $p(C_{60}^+) = 0.3\%$–0.9% from two diffuse interstellar bands at 958 and 963 nm which they attribute to C_{60}^+. Herbig (2000) uses these same two bands to estimate $p(C_{60}^+) = 0.1\%$–0.3% in diffuse clouds. Herbig (2000) places an upper limit of $p(C_{60}) < 0.0008\%$ in diffuse clouds, showing that C_{60} is primarily ionized in diffuse clouds. Moutou et al. (1999) measure $p(C_{60}) < 0.3\%$ and $p(C_{60}^+) < 0.3\%$ from the lack of emission features at 7.0–8.5 μm, at a position in NGC 7023 where the 18.9 μm C_{60} feature is weak. Nuccitelli et al. (2005) find $p(C_{60}) < 0.6\%$ from their non-detection of the 8.5 μm feature in absorption toward R CrB (HR 5880) and three massive young stellar objects. Cami et al. (2010) derive $p(C_{60}) = 1.5\%$ in planetary nebula Tc 1.

The relative intensities of the C_{60} bands provide information on the conditions in which the molecule emits. To probe these conditions, we use a Monte Carlo code, based on a micro-canonical formalism, developed to simulate the emission cascade of PAHs following the absorption of a UV photon (Joblin et al. 2002; Mulas et al. 2006). We calculate the evolution of the internal energy in the molecule and the number of photons emitted in each infrared band during the cooling cascade. We calculate the emission spectrum after C_{60} absorbs a 5, 10, or 15 eV photon, reaching temperatures of 800, 1200, or 1570 K at the beginning of the cooling cascade. We use the list of modes from Ménendez & Page (2000) and infrared intensities (at 0 K) calculated using density functional theory (Choi et al. 2000; Schettino et al. 2001).

We compare the predicted line intensities with the observations in Table 1. We find that the ratio of the intensities of the 17.4 and 18.9 μm bands is not sensitive to the energy of the absorbed UV photon. The observed ratio varies but this is likely because the 17.4 μm band is blended with a PAH feature. The ratio of the intensities of the 7.04 and 18.9 μm bands, however, is very sensitive to the absorbed UV photon energy. Table 1 shows that the 7.04 μm intensity in NGC 7023 is consistent with the cooling cascade of C_{60} excited by UV photons with a mean energy of 10 eV. A lower photon energy is suggested for NGC 2023, perhaps because of its blister geometry with the star in front of a dense molecular cloud. If C_{60} in NGC 2023 is excited by lower energy photons, then this would also affect the C_{60} abundance derived there. More detailed modeling will be needed to clarify this.

Our interpretation of the NGC 7023 C_{60} emission differs from the very recent results of Cami et al. (2010) who concluded that

C_{60} in Tc 1 emits in solid phase at a temperature of 330 K. Their analysis, however, is based on an excitation diagram to derive a single emission temperature, which is not appropriate to describe the cooling cascade of UV-excited molecules.

5. CONCLUSIONS

We confirm our identification of the 17.4 and 18.9 μm emission features in NGC 7023 with C_{60} (Werner et al. 2004b; Sellgren et al. 2007) by detecting a predicted emission feature at 7.04 $\pm$ 0.05 μm. We also detect 7.04, 17.4, and 18.9 μm emission features in NGC 2023. We demonstrate that the 17.4 μm emission feature in NGC 7023 is a blend of C_{60} and PAH emission with *Spitzer* imaging spectroscopy. Our work (Werner et al. 2004b; Sellgren et al. 2007; this Letter) is the first firm detection of neutral C_{60} in interstellar space.

We find that the infrared emission in NGC 7023 is consistent with the emission of gas-phase C_{60} excited by UV photons. Further modeling is required to explain the observations of NGC 2023. The percentage of interstellar carbon in C_{60} is 0.1%–0.6% in NGC 7023. This is consistent with previous estimates of, and limits on, the interstellar C_{60} and C_{60}^{+} abundances.

We thank Nick Abel, Lou Allamandola, Bruce Draine, Alain Léger, and Farid Salama for useful conversations, Dominique Toublanc for support with the Monte Carlo code, and Mike Jura for suggesting the C_{60} identification. This work is based on observations made with the *Spitzer Space Telescope*, which is operated by the Jet Propulsion Laboratory, California Institute of Technology, under a contract with NASA. Support for this work was provided by NASA through an award issued by JPL/Caltech.

Facilities: Spitzer (IRS)

REFERENCES

Bettens, R. P. A., & Herbst, E. 1996, ApJ, 468, 686
Bettens, R. P. A., & Herbst, E. 1997, ApJ, 478, 585
Boersma, C., Bauschlicher, C. W., Allamandola, L. J., Ricca, A., Peeters, E., & Tielens, A. G. G. M. 2010, A&A, 511, A32
Cami, J., Bernard-Salas, J., Peeters, E., & Malek, S. E. 2010, Science, 329, 1180
Cherchneff, I., Le Teuff, Y. H., Williams, P. M., & Tielens, A. G. G. M. 2000, A&A, 357, 572
Choi, C. H., Kertesz, M., & Mihaly, L. 2000, J. Phys. Chem. A, 104, 102
Clayton, D. D., Deneault, E. A.-N., & Meyer, B. S. 2001, ApJ, 562, 480
Clayton, G. C., Kelly, D. M., Lacy, J. H., Little-Marenin, I. R., Feldman, P. A., & Bernath, P. F. 1995, AJ, 109, 2096
Foing, B. H., & Ehrenfreund, P. 1994, Nature, 369, 296
Frum, C. I., Engleman, R. J., Hedderich, H. G., Bernath, P. F., Lamb, L. D., & Huffman, D. R. 1991, Chem. Phys. Lett., 176, 504
Goeres, A., & Sedlmayr, E. 1992, A&A, 265, 216
Herbig, G. H. 2000, ApJ, 542, 334
Houck, J. R., et al. 2004, ApJS, 154, 18
Jenniskens, P., Mulas, G., Porceddu, I., & Benvenuti, P. 1997, A&A, 327, 337
Joblin, C., Léger, A., & Martin, P. 1992, ApJ, 393, L79
Joblin, C., Toublanc, D., Boissel, P., & Tielens, A. G. G. M. 2002, Mol. Phys., 100, 3595
Kroto, H. W., Heath, J. R., O'Brien, S. C., Curl, R. F., & Smalley, R. E. 1985, Nature, 318, 162
Kroto, H. W., & Jura, M. 1992, A&A, 263, 275
Lambert, D. L., Rao, N. K., Pandey, G., & Ivans, I. I. 2001, ApJ, 555, 925
Li, A., & Draine, B. T. 2001, ApJ, 554, 778
Maier, J. P. 1994, Nature, 370, 423
Ménendez, J., & Page, J. B. 2000, in Light Scattering in Solids VIII: Fullerenes, Semiconductor Surfaces, Coherent Phonons, ed. M. Cardona & G. Güntherodt (Berlin: Springer), 27
Misawa, T., Gandhi, P., Hida, A., Tamagawa, T., & Yamaguchi, T. 2009, ApJ, 700, 1988
Moutou, C., Sellgren, K., Verstraete, L., & Léger, A. 1999, A&A, 347, 949
Moutou, C., Verstraete, L., Léger, A., Sellgren, K., & Schmidt, W. 2000, A&A, 354, L17
Mulas, G., Malloci, G., Joblin, C., & Toublanc, D. 2006, A&A, 460, 93
Nuccitelli, D., Richter, M. J., & McCall, B. J. 2005, in IAU Symp. 235, Astrochemistry: Recent Successes and Current Challenges, Poster Book, ed. A. J. Markwick-Kemper (Cambridge: Cambridge Univ. Press), 236
Pascoli, G., & Polleux, A. 2000, A&A, 359, 799
Schettino, V., Pagliai, M., Ciabini, L., & Cardini, G. 2001, J. Phys. Chem. A, 105, 11192
Scott, A., Duley, W. W., & Pinho, G. P. 1997, ApJ, 489, L193
Sellgren, K., Uchida, K. I., & Werner, M. W. 2007, ApJ, 659, 1338
Smith, J. D. T., et al. 2007a, ApJ, 656, 770
Smith, J. D. T., et al. 2007b, PASP, 119, 1133
Snow, T. P., & Seab, C. G. 1989, A&A, 213, 291
Sogoshi, N., Kato, Y., Wakabayashi, T., Momose, T., Tam, S., DeRose, M. E., & Fajardo, M. E. 2000, J. Phys. Chem. A, 104, 3733
Somerville, W. B., & Bellis, J. G. 1989, MNRAS, 240, 41P
Tielens, A. G. G. M. 2008, ARA&A, 46, 289
Velusamy, T., & Langer, W. D. 2008, AJ, 136, 602
Werner, M. W., Uchida, K. I., Sellgren, K., Marengo, M., Gordon, K. D., Morris, P. W., Houck, J. R., & Stansberry, J. A. 2004b, ApJS, 154, 309
Werner, M. W., et al. 2004a, ApJS, 154, 1
Yagi, H., et al. 2009, Carbon, 47, 1152
Yasumatsu, H., Kondow, T., Kitagawa, H., Tabayashi, K., & Shobatake, K. 1996, J. Chem. Phys., 104, 899